infrastructures

MDPI

Article

Modeling Pavement Deterioration on Nepal's National Highways: Integrating Rainfall Factor in a Hazard Analysis

Manish Man Shakya [1,2,*], Kotaro Sasai [1], Felix Obunguta [1], Asnake Adraro Angelo [1] and Kiyoyuki Kaito [1]

1 Department of Civil Engineering, Osaka University, 2-1 Yamadaoka, Suita, Osaka 565-0871, Japan; k.sasai@civil.eng.osaka-u.ac.jp (K.S.); f.obunguta@civil.eng.osaka-u.ac.jp (F.O.); angelo@civil.eng.osaka-u.ac.jp (A.A.A.); kaito@ga.eng.osaka-u.ac.jp (K.K.)

2 Department of Roads, Ministry of Physical Planning and Transport, Babarmahal, Kathmandu 44600, Nepal

* Correspondence: shakya.m@civil.eng.osaka-u.ac.jp or 28j22803@gmail.com

Abstract: Pavement deterioration is influenced by various factors with degradation rates varying widely depending on the type of pavement, its use, and the environment in which it is located. In Nepal, where the climate varies from alpine to subtropical monsoon, understanding pavement degradation is essential for effective road asset management. This study employs a Markov deterioration hazard model to predict pavement deterioration for the national highways managed by Nepal's Department of Roads. The model uses Surface Distress Index data from 2021 to 2022, with traffic and cumulative monsoon rainfall as explanatory variables. Monsoon rainfall data from meteorological stations were interpolated using Inverse Distance Weighted and Empirical Bayesian Kriging 3D methods for comparative analysis. To compare the accuracy of interpolated values from the IDW and EBK3D methods, error metrics such as Mean Absolute Error (MAE), Root Mean Squared Error (RMSE), and Mean Bias Error (MBE) were employed. Lower values for MAE, RMSE, and MBE indicate that EBK3D, which accounts for spatial correlation in three dimensions, outperforms IDW in terms of interpolation accuracy. The monsoon rainfall interpolated values using the EBK3D method were then used as an explanatory variable in the Markov deterioration hazard model. The Bayesian estimation method was applied to estimate the unknown parameters. The study demonstrates the potential of integrating the Markov deterioration hazard model with monsoon rainfall as an environmental factor to enhance pavement deterioration modeling. This model can be adapted for regions with a similar monsoon climate and pavement types making it a practical framework for supporting decision-makers in strategic road maintenance planning.

Keywords: pavement deterioration; road asset management; Markov deterioration hazard model; exponential hazard function; IDW interpolation; EBK3D interpolation

1. Introduction

Pavement deterioration is a significant challenge in road asset management, especially in developing countries like Nepal, where varying climatic conditions mixed with high traffic volumes challenge maintenance strategies. Effective road asset management aims to minimize the life cycle costs of road infrastructure by ensuring timely inspections, accurate predictions of degradation, and the implementation of periodic maintenance measures. However, predicting pavement deterioration in regions with complex environmental variables, such as monsoons and diverse topography, requires advanced analytical approaches.

In Nepal, the road network of national highways, feeder roads, and sub-urban roads is collectively termed the Strategic Road Network (SRN). Maintaining these roads is par-

ticularly challenging due to Nepal's topography and diverse climate, which ranges from alpine in the Himalayas to temperate and subtropical monsoon climates in the mid-hills and plains [1]. In Nepal, the majority of rainfall events occur during the monsoon season, accounting for about 80% of the yearly rainfall from June to September [2,3]. This intense and prolonged precipitation significantly affects road conditions, expediting pavement deterioration and imposing challenges to traffic safety and maintenance planning. The Department of Roads (DOR) conducts annual road maintenance planning to maintain the SRN in serviceable condition. However, as this method does not enable pavement condition prediction, it is challenging to implement long-term maintenance planning, which is essential for effective asset management and strategic decision-making concerning budget allocation and road network performance. To address these challenges, predictive models that consider both traffic and environmental factors are essential. However, such pavement deterioration models specifically developed for Nepal's unique traffic and climatic conditions are not available in practice.

In light of these limitations, relying on various pavement prediction models becomes essential for effective long-term planning. Referring to pavement management guidelines, commonly utilized models for predicting pavement conditions include deterministic, probabilistic, Bayesian, and expert-based methods [4]. This study adopts Markov deterioration hazard models, a probabilistic approach, to study pavement deterioration while considering the impact of traffic and environmental factors. The term 'hazard' in the pavement deterioration model refers to the instantaneous probability rate of deterioration over time.

The monsoon is considered as the environmental explanatory variable. The value assigned for the road section under study is the interpolated value based on the rainfall measurement from meteorological stations. This study also compares the effectiveness of two interpolation techniques, (a) Inverse Distance Weighted (IDW) and (b) Empirical Bayesian Kriging 3D (EBK3D), for estimating monsoon parameters. These methods enable the distribution of Cumulative Monsoon Rainfall (CMR) data to be integrated into the Markov model as an explanatory variable, enhancing the predictive accuracy of pavement deterioration forecasts.

From an academic perspective, predicting pavement deterioration in a developing country like Nepal presents significant challenges due to limited data availability and considerable variability in environmental and traffic factors. Although Tsuda et al. (2006) [5] have provided a robust foundation with the Markov deterioration hazard model, its application to road pavements in South Asia, where climatic conditions such as monsoons having significant influence, remain underexplored. This study attempts to address these gaps by applying a Markov deterioration hazard model to Nepal's road network and climatic conditions. This study seeks to provide valuable insights that can enhance pavement deterioration prediction not only in Nepal but also in other regions with similar climatic and infrastructure challenges.

2. Literature Review

DOR, established in 1962, is a government institution responsible for the development and upkeep of the SRN through its various construction projects and maintenance divisions [6]. The necessary funds for repair and maintenance of the SRN are provided by the Roads Board Nepal (RBN) to various road division offices. Using the RBN fund, the DOR conducts road pavement condition surveys every year. Pavement performance indicators such as the Surface Distress Index (SDI) and International Roughness Index (IRI) are recorded. Similarly, traffic data in the road network are measured as Annual Average Daily Traffic (AADT). Using these data, the process for planning and prioritizing the various maintenance strategies is prepared by DOR in the form of an integrated annual

road maintenance plan to be executed in the following fiscal year for all road maintenance division offices under DOR [7]. The approach for planned maintenance and the detailed guidelines for road screening and ranking are outlined in the "Standard Procedure for Periodic Maintenance Planning", published by the DOR Maintenance Branch in November 2005. This policy document considers the SDI as the key pavement performance parameter [7]. Although the present annual road maintenance plan supports the maintenance plan for a year, it is essential to have a comprehensive road asset management system to support long-term maintenance planning.

The Highway Development and Management (HDM-4) model is a widely recognized deterministic tool used for predicting pavement deterioration. Neighboring countries like Bangladesh and India also use HDM-4 for pavement maintenance planning. The Department of Roads and Highways in Bangladesh uses HDM-4 as part of its Road Maintenance and Management System [8]. Similarly, in India, HDM-4 is used for road deterioration prediction over time and under varying traffic and environmental conditions [9]. Moreover, HDM-4 is a deterministic model, and it is necessary to calibrate HDM-4 deterioration models to adapt to the specific traffic characteristics, terrain, soil types, climatic conditions, and pavement composition of the region where they are applied. Additionally, implementing HDM-4 poses challenges in many developing countries, where budget constraints, calibration in application, verification, and adaptation level for the long term make it difficult to meet the method's high data requirements [9,10].

However, probabilistic models are suitable for scenarios where variability and uncertainty are high such as pavement deterioration prediction. Tsuda et al. (2006) introduced a Markov deterioration hazard model for predicting pavement deterioration that has been widely referenced for its ability to model deterioration processes [5]. Kobayashi et al. (2010) expanded on this by integrating Bayesian estimation methods to improve the robustness of deterioration forecasts [11,12]. These studies provide a strong foundation for applying Markov models to pavement management systems, making it an essential tool in the context of pavement management systems.

Environmental factors, particularly rainfall, significantly contribute to accelerated pavement deterioration. The distress in bituminous pavement is induced by moisture damage in the forms of raveling, potholes, etc., resulting from intense rainfall [13]. In Nepal, monsoon rainfall is predominant [2,3,14], leading to increased moisture infiltration into the underlying pavement layer, weakened subgrade support, and subsequent surface distress. The rainwater penetrates pavement cracks and weakens the underlying layers. Pavement damage caused by rainwater accompanied by poor drainage is particularly pronounced in wet climates and areas subject to freezing [15]. The increase in moisture in the underlying layer increases both the fatigue strain and the permanent deformation strain of the pavement [16]. Excessive rainfall can lead to increased roughness, which results in faster deterioration rates and reduced service life [17]. The Department of Hydrology and Meteorology (DHM) in Nepal operates a network of hydrological and meteorological stations that records essential environmental data, which can be analyzed to study its impact on infrastructure [18]. However, the uneven location of meteorological stations and the fact that rainfall data from the meteorological stations are not specifically collected for road infrastructure make it challenging to directly assign to specific road sections. To overcome this limitation, spatial interpolation techniques are essential to accurately estimate unknown rainfall values for corresponding road sections and assign them as an explanatory variable in pavement deterioration predictive models.

To estimate the monsoon rainfall distribution across Nepal, this study applies two interpolation methods, IDW and EBK3D, which are widely used in hydrological and environmental studies [19–21]. IDW is a simple and widely used deterministic method

that assigns weights to known data points such that closer data points have a greater influence on the estimated value. However, it does not consider spatial correlations, limiting its effectiveness in complex terrains [22]. Conversely, EBK3D extends traditional kriging [23] into three dimensions, incorporating a Bayesian framework that accounts for uncertainty in variogram estimation and improves the interpolation accuracy for complex data distributions [21,24].

3. Methodology

This study employs a Markov deterioration hazard model to predict pavement deterioration, integrating environmental data, particularly CMR on road surfaces. The more accurate values obtained from two distinct interpolation techniques, (a) IDW and (b) EBK3D, to model environmental data are used to model the environmental data in this study. Figure 1 illustrates the framework for pavement deterioration modeling using the Markov deterioration hazard model. The methodology is structured into four main stages: data collection, data preprocessing, interpolation of rainfall data, and application of the Markov deterioration hazard model with Bayesian parameter estimation.
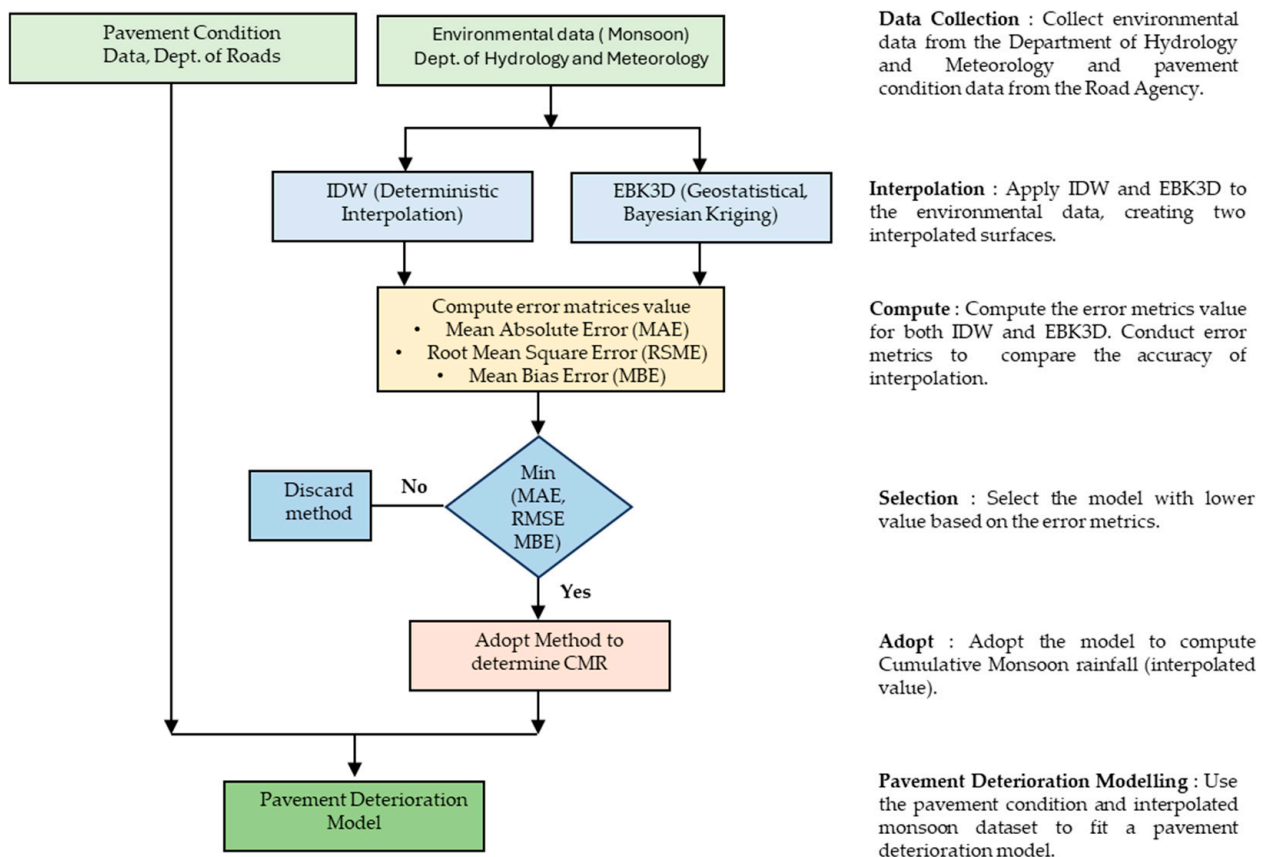

Figure 1. Pavement Deterioration Modeling Framework.

3.1. Data Collection

The data utilized in this study were collected from periodic inspection reports recorded in the road register of the Highway Management Information System (HMIS) at DOR. This dataset includes information on pavement conditions and traffic volumes. Additionally, daily rainfall data was sourced from meteorological stations managed by the DHM.

3.1.1. Surface Distress Index (SDI)

DOR considers surface distress of pavement as an important indicator for assessing pavement performance and ensuring it meets the road's serviceability requirements. SDI quantifies pavement distress, including cracks, disintegration (potholes), deformations, texture deficiency, pavement edge defects, and other forms of deterioration. In the context of Nepal, civil engineers specializing in highways and pavement specialists perform inspections and measurements to assess and quantify pavement distress for each 1 km road section. These data are then used to compute the SDI value for the surveyed road section. The method for determining the SDI value and interpretation of the results can differ based on the surveyor's judgment and expertise and the guidelines established by the respective road agencies.

DOR in Nepal adopts a six-level rating index, ranging from 0 to 5 for quantifying the surface distress using SDI. A rating of 0 represents a pavement surface without any defect whereas a rating of 5 represents the maximum possible defects. This rating scale was recommended by the World Bank and has been modified to address the requirement of DOR. The methodology for measurement of SDI is outlined in "Road Pavement Management, MRCU" [25].

3.1.2. Traffic Data

Traffic data are acquired from HMIS and DOR. The classified traffic count survey includes the counting and analysis of motorized and non-motorized vehicles at 160 traffic count stations located at the major junctions on the SRN of Nepal. The traffic data are represented as AADT expressed in Passenger Car Units (PCUs) and utilized as an explanatory variable in the hazard model.

3.1.3. Rainfall Data

Rainfall data are acquired from the daily rainfall records of meteorological stations managed by DHM in Nepal. These stations are primarily established to monitor various parameters, including river hydrology, water quality, sedimentation, limnology, snow hydrology, glaciology, weather, climate, agro-meteorology, air quality, and solar energy [26]. The cumulative sums of rainfall during the monsoon period (July–September) recorded by these stations are interpolated and assigned to the road section and utilized as an explanatory variable in the hazard model.

3.2. Data Processing

Data preprocessing involves cleaning and organizing the datasets to ensure compatibility for analysis. The Markov deterioration hazard model has two assumptions, which are outlined in Section 3.4. Road sections not satisfying Markov assumption and with missing traffic data or rainfall records are excluded to ensure consistency. The explanatory variables (e.g., AADT and CMR) are normalized to their maximum values to facilitate parameter and assigning rainfall data to road sections using spatial interpolation methods.

3.3. Rainfall Interpolation Techniques

Two interpolation techniques are used to distribute rainfall data spatially across the road network preprocessing involves cleaning and organizing the datasets to ensure compatibility for analysis.

3.3.1. Inverse Distance Weighted (IDW) Interpolation Interpolation

The IDW interpolation method is a deterministic technique widely used to estimate unknown values at a given location based on nearby known values. These known values are weighted inversely by their distance from the target location, meaning that closer points

have a stronger influence on the predicted value than distant points. To estimate the value at an unmeasured location, IDW utilizes the measured values surrounding the prediction location [22]. The generalized equation for IDW is:

$$Z(x_o) = \frac{\sum_{i=1}^{N} Z(x_i).d_i^{-p}}{\sum_{i=1}^{N} d_i^{-p}} \tag{1}$$

where:

$Z(x_o)$ = the interpolated value at the target location x_o.

$Z(x_i)$ = the known value at the ith location.

d_i = the distance between the ith known point and the target location x_o.

N = the number of known stations used for interpolation

p = the power parameter, which influences the weighting of known values. As the distance between the prediction location and the measured locations increases, the influence of each measured point on the prediction decreases exponentially.

3.3.2. Empirical Bayesian Kriging 3D (EBK3D) Interpolation

EBK3D is a geostatistical interpolation method that extends kriging into three-dimensional space. The variogram in EBK3D characterizes the spatial dependency structure of the data, allowing the interpolation to consider both the distance and spatial correlation between points. A Bayesian framework is used to account for uncertainty in variogram estimation, enhancing the accuracy of the variogram estimates [21]. The generalized equation for EBK is:

$$Z(s_X) = \sum_{i=1}^{N} \lambda_i Z(s_i) \tag{2}$$

where:

$Z(s_i)$ = the measured value at the ith location

$Z(s_X)$ = the interpolated value at a known location

N = the number of measured values

λ_i = the weights assigned to each known point. These weights are calculated by integrating information from semivariograms that are generated from the datasets. For the semivariograms, it is essential to compute the semi-variance using Equation (4). The details of which are explained in the following section.

The coordinates s_i and s_X represents 3D locations, i.e., (x, y, z). The semivariogram model is calculated in 3D, accounting for spatial autocorrelation in all three dimensions. The estimation involves calculating the distances in 3D space:

$$h_{ij} = \sqrt{(x_i - x_j)^2 + (y_i - y_j)^2 + (z_i - z_j)^2} \tag{3}$$

where, h_{ij} represents the 3D distance between two s_i and s_j.

Semi-Variance

Semi-variance is a statistical measure of the dissimilarity between two spatial points separated by a certain distance. It quantifies how similar (or different) two points are based on their values. The general formula for semi-variance is given by:

$$\gamma(h) = \frac{1}{2N(h)} \sum_{i=1}^{N(h)} [Z(s_i) - Z(s_i + h)]^2 \tag{4}$$

where:

$\gamma(h)$ = semivariance for a given lag distance h.

$N(h)$ = number of pairs of points that are separated by a distance h.

$Z(s_i)$ = value at location s_i.

$Z(s_i + h)$ = value at a location separated from s_i by a distance h. The lag distance (h) is the interval used to group point pairs for calculating semi-variance.

Semivariogram

A semivariogram is a plot of semi-variance (a measure of dissimilarity) on the y-axis and lag distance on the x-axis that shows how the semi-variance between pairs of points changes with increasing distance. The semivariogram helps describe the spatial autocorrelation of a dataset, showing how related data points are based on their separation distance. It provides insights into how variability between data points changes with distance [23].

A simple semivariogram is shown in Figure 2a. The red dots (points) represent the calculated semi-variance $\gamma(h)$ values corresponding to each lag distance h. The green curve represents the best-fit semivariogram. There are three components of a semivariogram.
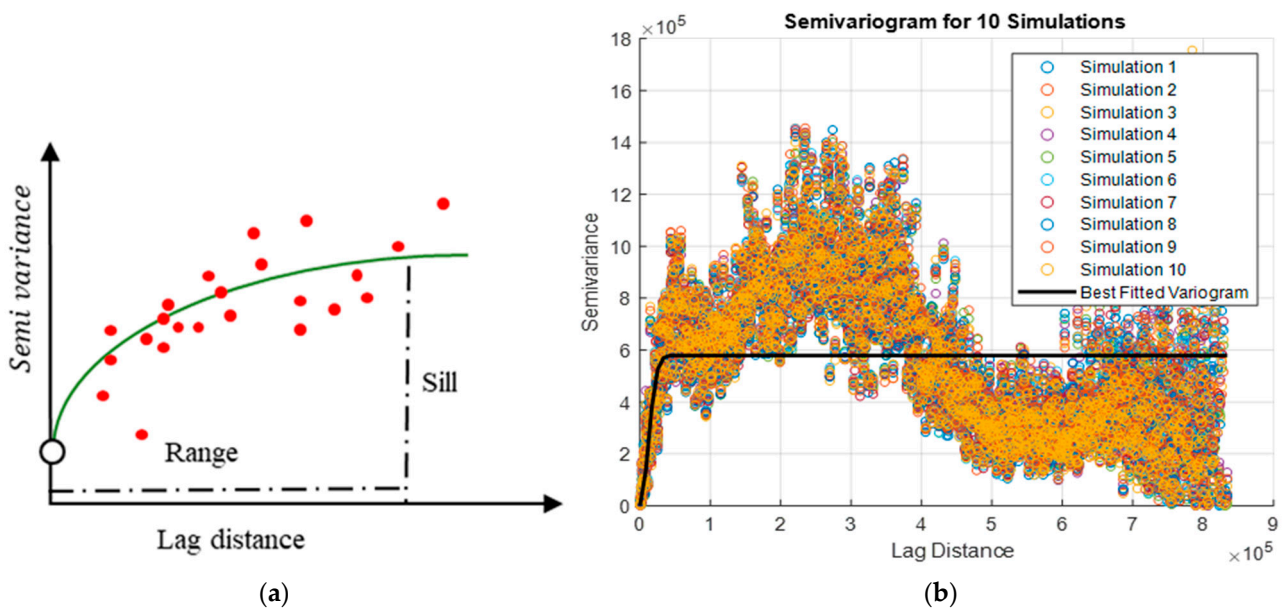

Figure 2. (**a**) A simple semivariogram; (**b**) The EBK model semivariograms.

1. Nugget (C_o): The value where the semivariogram intercepts the y-axis. This represents spatial variability at very small scales or measurement errors.
2. Range (a): The distance beyond which points are no longer spatially correlated.
3. Sill (C): The value of the semi-variance at which the semivariogram levels off. This represents the point where adding more distance between points does not increase variability further.

Similarly, semivariogram modeling in the EBK method involves multiple simulations to form a variogram spectrum, and the best-fit variogram model is computed to determine the nugget, sill, and range values. The prime advantage of EBK3D is that it automatically calculates these components through a process of sub-setting and simulations requiring minimal intervention [21]. Figure 2b. illustrates an example of the best-fit variogram model for rainfall data recorded by 422 rainfall stations all over Nepal in 2021. The values C_o, a, and C derived from the EBK method using Equation (4) are used to fit the theoretical

exponential semivariogram model. This model estimates the semi-variance value $\gamma(h)$ at lag distance h using the formula:

$$\gamma(h) = C_o + C\left(1 - e^{-\frac{3h}{a}}\right) \tag{5}$$

Referring to Equation (2), to obtain the value for λ_i, we need to solve the linear system:

$$K \cdot \lambda_i = X \tag{6}$$

$$\begin{bmatrix} \gamma(h_{11}) & \gamma(h_{12}) & & \gamma(h_{1N}) & 1 \\ \gamma(h_{21}) & \gamma(h_{22}) & \cdots & \gamma(h_{2N}) & 1 \\ \vdots & \vdots & \ddots & \vdots & 1 \\ \vdots & \vdots & & \vdots & 1 \\ \gamma(h_{N1}) & \gamma(h_{N2}) & \cdots & \gamma(h_{NN}) & 1 \\ 1 & 1 & & 1 & 0 \end{bmatrix} * \begin{bmatrix} \lambda_1 \\ \lambda_2 \\ \vdots \\ \vdots \\ \lambda_N \\ \end{bmatrix} = \begin{bmatrix} \gamma(h_{1X}) \\ \gamma(h_{2X}) \\ \vdots \\ \vdots \\ \gamma(h_{NX}) \\ 1 \end{bmatrix} \tag{7}$$

In Equation (6), K is the kriging matrix and each element $\gamma(h_{ij})$ is the semivariogram value between the two points i and j computed by using Equation (5), such that $\gamma(h_{12}) = \gamma(h_{21})$ and $\gamma(h_{11}) = \gamma(h_{22}) = \gamma(h_{NN}) = \gamma(0) = 0$. The values for λ_i can be computed by rearranging Equation (6) as $\lambda_i = K' \cdot X$.

Similarly, $[\lambda_1, \lambda_2, \ldots \lambda_N]$ are the weights assigned such that the value $[\lambda_1, \lambda_2, \ldots \lambda_N]$ will be between 0 and 1 and their sum will be 1. is the Lagrange multiplier used to ensure that the sum of weights is 1.

3.3.3. Error Metrics and Comparision

Error metrics are statistical measures used to evaluate the accuracy of a predictive model by quantifying the differences between observed O_i ($i = 1, 2, \ldots, n$) and predicted P_i ($i = 1, 2, \ldots, n$) values, where n is the number of the observation. Individual method prediction errors E_i are usually defined as $E_i = P_i - O_i$. Common error metrics used to compare between the methods are the following:

Mean Absolute Error (MAE)

MAE represents the average magnitude of errors between observed and predicted values, considering all differences without taking their direction into account. In simple terms, it tells us how far the model's predictions are from the actual values on average. The general formula for MAE is:

$$MAE = \frac{1}{n}\sum_{i=1}^{n}|E_i| \tag{8}$$

Lower MAE values indicate better model performance, meaning the model's predictions are closer to the observed values. Since MAE has the same units as the observed values, it is scale-dependent and is directly interpretable in the context of the data being evaluated [27].

Root Mean Square Error (RMSE)

RMSE measures the square root of the average squared differences between observed and predicted values. The general formula for RMSE is:

$$RMSE = \frac{1}{n}\sum_{i=1}^{n}(E_i)^2 \tag{9}$$

RMSE gives more emphasis on larger errors by squaring the error. Lower values of RMSE indicate better model accuracy [27].

Mean Bias Error (MBE)

MBE represents the average difference between observed and predicted values, indicating the model's bias. The general formula for RMSE is:

$$MBE = \frac{1}{n}\sum_{i=1}^{n}(E_i) \tag{10}$$

An MBE value close to zero indicates little bias, whereas a positive or negative value suggests that the model tends to systematically overestimate or underestimate, respectively [27].

3.4. Markov Deterioration Hazard Model Formulation

The Markov deterioration hazard model is a probabilistic model to predict the pavement condition transition based on survival analysis and hazard function. It assumes that (a) during the inspection period no maintenance activities were carried out and no measurement error occurred and (b) the deterioration of the road infrastructure is a natural process and its condition gradually degrades over time [5].

The road infrastructure deterioration process and periodic inspection of condition states are illustrated graphically in Figure 3. Here, the y-axis is real calendar time (in short, time) denoted by the symbol τ. The deterioration of the road pavement starts immediately after the construction is completed and the road is opened to traffic at an initial time τ_0. The condition state of a pavement section is expressed by a rank J representing a state variable i ($i = 1, 2, \ldots, J$). For a new pavement, $i = 1$, and the state variable j is assumed to increase as deterioration progresses. A value of $i = J$ indicates that a pavement section has reached the end of its service life.
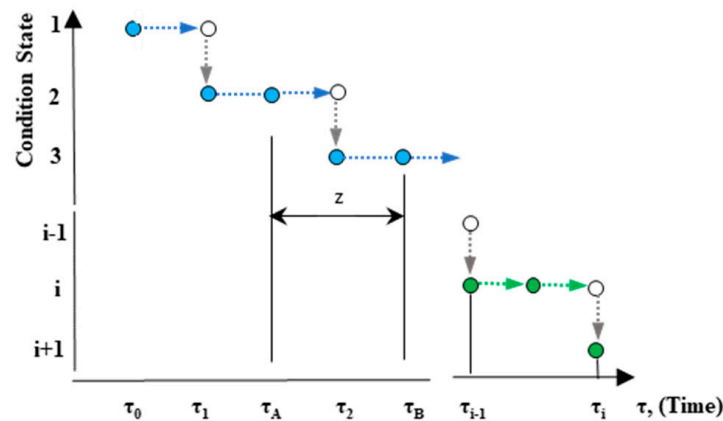

Figure 3. Periodic inspection of condition states.

The information corresponding to the deterioration process of a pavement can be obtained from periodic inspections. For simplicity, two periodic inspections are conducted at times τ_A and τ_B, at a time interval of z. It is supposed that at time τ_A, the condition state observed during the inspection is i ($i = 1, 2, \ldots, J - 1$). It is difficult to obtain information about the time at which the transition to the observed condition state occurred i.e., τ_1 and τ_2.

The transition process of the condition state for road pavement is uncertain and forecasting future condition state cannot be determined deterministically. Assuming that the deterioration process follows the Markov chain, the Markov transition probability (MTP) is

employed to represent the uncertainty in condition state transitions over two time points. In other words, MTP is utilized to predict pavement deterioration based on the periodic inspection process as illustrated in Figure 3.

Let us suppose that during periodic inspections at time τ_A, the observed condition state of the road pavement is i. This is represented by the condition state variable $h(\tau_A) = i$. Then, the Markov transition probability π_{ij} is defined as the probability that given a condition state $h(\tau_A) = i$ observed at time τ_A will transition to $h(\tau_B) = j$ at a future time τ_B. Mathematically, it is expressed as:

$$\text{Prob}[h(\tau_B) = j | h(\tau_A) = i] = \pi_{ij} \tag{11}$$

By deriving the pair of states (i, j) from a transition probability, we can obtain the MTP matrix $\prod$, which is expressed as:

$$\prod = \left(\begin{bmatrix} \pi_{11} & \cdots & \pi_{1J} \\ \vdots & \ddots & \vdots \\ 0 & \cdots & \pi_{JJ} \end{bmatrix} \right) \tag{12}$$

Regarding the MTP, the following must hold true:

$$\pi_{ij} \geq 0 \ (i, j = 1, \ldots, j)$$

$$\pi_{ij} = 0 \ (\text{when } i > j) \text{ and}$$

$$\sum_{j=1}^{J} \pi_{ij} = 1.$$

The condition state J is the absorbing state in the Markov chain if there is no repair, thus $\pi_{JJ} = 1$ is true. Moreover, the MTP is independent of past deterioration records and is dependent only on the condition state at the time of inspection.

Estimation of MTP

The MTPs based on the exponential hazard model are defined in the following equations.

$$\pi_{i\,i} = \text{Prob}[h(y_B) = i \mid h(y_A) = i] = \exp(-\theta_i Z) \tag{13a}$$

$$\pi_{i\,i+1} = \text{Prob}[h(y_B) = i + 1 \mid h(y_A) = i]$$

$$= \frac{\theta_i}{\theta_i - \theta_{i+1}} \{ -\exp(-\theta_i Z) + \exp(-\theta_{i+1} Z) \} \tag{13b}$$

$$\pi_{ij} = \text{Prob}[h(y_B) = j \mid h(y_A) = i]$$

$$= \sum_{k=i}^{j} \prod_{m=i}^{k-1} \frac{\theta_m}{\theta_m - \theta_k} \prod_{m=k}^{j-1} \frac{\theta_m}{\theta_{m+1} - \theta_k} \exp(-\theta_k Z) \tag{13c}$$

where,

$$\prod_{m=i}^{k-1} \frac{\theta_m}{\theta_m - \theta_k} = 1, \ at(k \leq i+1) \text{and}$$

$$\prod_{m=k}^{j-1} \frac{\theta_m}{\theta_{m+1} - \theta_k} = 1 \ at \ (k \geq j).$$

In Equation (13c), $\pi_{ij}\left[0 < \pi_{ij} < 1\right]$, and π_{iJ} is structured according to the MTP conditions as follows:

$$\pi_{iJ} = 1 - \sum_{j=1}^{j-1} \pi_{ij} \tag{13d}$$

Equations (13a)–(13d) defines the multistage exponential hazard model. In this model, the hazard rate $\theta_i^k (i = 1, 2, \ldots, J-1); k = 1, \ldots, K)$ representing the deterioration process of a road pavement section is considered to change in relation to explanatory variables x^k as follows:

$$\theta_i^k = exp\left(\boldsymbol{\beta}_{i,1} + \boldsymbol{\beta}_{i,2} x_2^k + \ldots, \boldsymbol{\beta}_{i,M} x_M^k\right) \tag{14}$$

$$\theta_i^k = f\left(\boldsymbol{x}^k : \boldsymbol{\beta}_i'\right) \tag{15}$$

where $\beta_i = (\beta_{i,1}, \ldots, \beta_{i,M})$ is a row vector of unknown parameters, $\beta_{i,m} = (m = 1, \ldots, M)$, and the symbol ' indicates the vector's transpose.

Briefly, the elements of MTP matrix π_{iJ} are estimated using dataset $\pi_{iJ}\left(Z^k, \boldsymbol{x}^k : \boldsymbol{\beta}_i\right)$, which can be obtained from inspection. The unknown parameter $\boldsymbol{\beta}_i$ $(i = 1, 2, \ldots, J-1)$ is determined using the Bayesian estimation method. For a detailed explanation of the Bayesian method for estimation, it is recommended to refer to Han D et al. [11]. Using Equation (15), the hazard function θ_i^k is estimated.

By using the obtained hazard function, the life expectancy (LE) of each condition state i is then defined by means of survival function $R_i\left(y_i^k\right)$. [28]

$$LE_i^k = \int_0^\infty \exp(-\theta_i^k y_i^k) dy_i^k = \frac{1}{\theta_i^k} \tag{16}$$

$$LE_i^J = \sum_{i=1}^{J-1} LE_i^k \tag{17}$$

The life expectancy from condition state i to J can be defined by the sum of life expectancies, and the deterioration curve can be attained by their relations. The MTP matrix $\prod$ as described in Equation (12) is derived by combining π_{ij} from Equations (13a)–(13d). For more details, it is suggested to refer to Tsuda et al., 2006 [5].

4. Empirical Analysis

For this empirical analysis, actual pavement inspection data for national highway road surfaces from DOR were employed. DOR currently manages 14,913 km of SRN and 2025 no. of motorable bridges. This excludes approximately 3,029 km of highways that are either under construction or planned [29,30]. Based on the pavement type, these road networks can be classified into two groups (i) surface treatment over a granular base (STGB) and (ii) asphalt material over a granular base (AMGB). In the annual road condition survey conducted in 2022, it was found that 88.45 percent of Nepal's national highways are paved with STGB pavement. STGB is a simple, highly effective, and cost-efficient road surface treatment provided that proper planning and execution of the work are followed during the construction [31].

The SDI data for national highways with STGB pavement, collected from the annual pavement inspection surveys for the years 2021 and 2022, were used in this study. The dataset confirms the assumptions of the Markov model were analyzed. A Bayesian estimation for the Markov deterioration hazard model was performed utilizing the actual inspection datasets, all based on SDI and each spanning 1 km. The inspection data consist of two condition states—an initial and a final state—as defined in Table 1. These states

serve as performance measures of road pavement distress, derived from two inspections conducted at specific intervals, denoted as Z, with explanatory variables, denoted as x.

Table 1. Road condition based on SDI.

| SDI Value	Condition	Incidence of Minor Defects	Incidence of Major Defects	Condition State
0	Good	None	None	1
1	Moderate	1 to 200 sq.m. per km.	1 occurrence	2
2	Satisfactory	<50% of the area	2 to 4 occurrences	3
3	Fair	≥50%	<30% of area	4
4	Poor		30% or potholes and base exposed <20% of the area	5
5	Bad		Potholes and exposed base = 20% of the area	6

In this study, monsoon rainfall is considered as the explanatory variable and is acquired from the daily records from DHM. DHM has established 579 meteorological stations and 110 hydrological stations to monitor all hydrological and meteorological activities across Nepal. To implement the Bayesian estimation for the Markov deterioration hazard model, the condition ratings presented in Table 1 were used to evaluate the pavement conditions based on the SDI values. Condition state 1 represents the best condition, while condition state 6 indicates the worst pavement condition.

In this study, CMR is considered an environmental explanatory variable. This is the sum of daily rainfall during the monsoon period. These values are interpolated using two interpolation techniques: IDW and EBK3D. Equation (1) is used with a power parameter (p) set to 2 for performing the IDW interpolation. A total of 422 of the 579 meteorological stations, each with a complete record of monsoon rainfall, are randomly divided into training and validation sets, containing 80 percent and 20 percent of the data, respectively. The CMR data from the training set of stations are used for interpolation and to determine the distribution of CMR over Nepal using the IDW and EBK3D methods. The CMR values at the validation set of stations are then predicted and compared with the actual measured values using error metrics. Lower values of MAE, RMSE, and MBE indicate that EBK3D, which incorporates spatial correlations in three dimensions, provides higher interpolation accuracy compared to IDW. Consequently, the interpolated CMR values obtained through the EBK3D method were utilized as an explanatory variable in the Markov deterioration hazard model.

The interpolated values are assigned to the road sections and the dataset $DS = [i, j, z, aadt, C_{m,EBK3D}]$ is prepared. Data for which information on traffic and CMR are not available were removed. The final database used for exponential hazard model estimation consisted of 5757 samples for DS. Furthermore, the explanatory variables were normalized to their maximum value to facilitate the estimation procedure. These datasets are utilized in this study to estimate the unknown parameter β, hazard rate, and life expectancies for each transition in condition state using Equations (14)–(17). Additionally, the pavement deterioration curve can be plotted to visually understand the deterioration process.

5. Results

The cumulative monsoon rainfall distribution for Nepal was generated using IDW and EBK3D interpolation with 2021 rainfall data, as depicted in Figures 4a and 4b, respectively. The results for the error metrics are shown in Table 2.
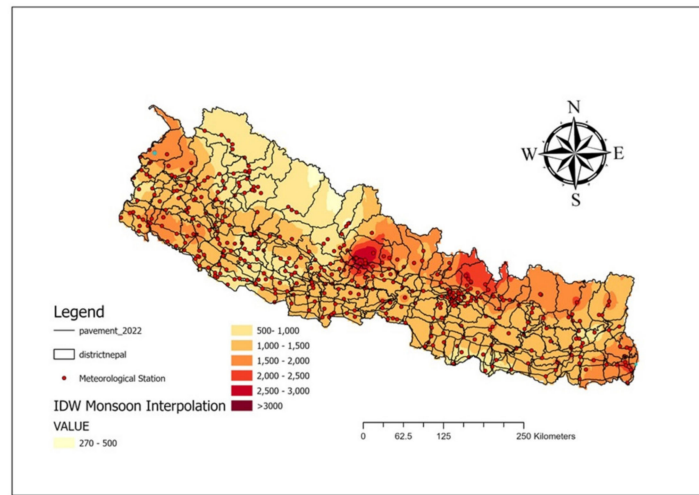
(a)
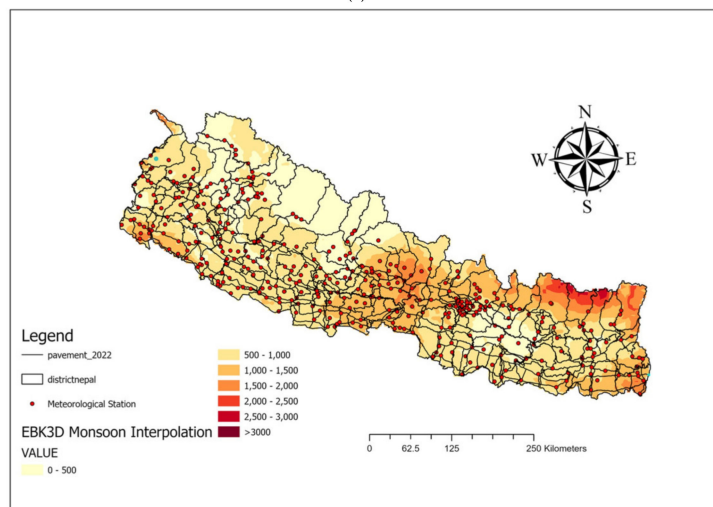
(b)

Figure 4. (**a**) SRN and Cumulative Monsoon Rainfall Distribution using IDW, mm, 2021; (**b**) SRN and Cumulative Monsoon Rainfall Distribution using EBK3D, mm, 2021.

Table 2. Error metric values.

S.No	Method	MAE	RMSE	MBE
1	IDW	454.66	616.57	145.95
2	EBK3D	421.90	588.32	121.17

Comparing the two interpolation methods, the lower values of MAE and RMSE for EBK3D indicate higher accuracy, and the lower value of MBE indicates minimal bias.

The interpolated value from the EBK3D interpolation method was assigned to the road sections as the explanatory variable. With the dataset structured as *DS*, the exponential hazard function was estimated separately. MTP matrixes for each sample were estimated using Equations (13a)–(13d). The average MTP matrix was determined in order to avoid the huge amount of individual estimations and is presented in Table 3. Since there is one exponential hazard function for each of the five ratings and each equation contains three unknown parameters, there are 15 unknown parameters $\beta = \{\beta_{i1}, \beta_{i1}, \beta_{i1} \ (i = 1, \dots, 5)\}$. Positive values of the unknown parameter β for the explanatory variable indicate a positive deteriorating effect on the pavement. For the datasets *DS*, the Bayesian estimates of the unknown parameter β are presented in Table 4, with each explanatory variable's corresponding Geweke's test value shown in parentheses.

Table 3. MTP Matrix—Model$_{EBK3D}$.

Rating	1	2	3	4	5	6
1	0.288	0.297	0.319	0.076	0.017	0.004
2	-	0.195	0.539	0.192	0.057	0.018
3	-	-	0.515	0.306	0.126	0.053
4	-	-	-	0.411	0.346	0.243
5	-	-	-	-	0.368	0.632
6	-	-	-	-	-	1.000

Table 4. Exponential Hazard Model Results—Model$_{EBK3D}$.

Rating	Absolute Term, β_0	AADT, β_{i1}	CMR, β_{i2}
1-2	0.718 (−1.116)	0.195 (1.558)	- -
2-3	0.618 (1.287)	1.043 (0.890)	- -
3-4	−0.704 (−1.021)	- -	0.869 (1.734)
4-5	−0.255 (1.011)	- -	0.443 (−1.069)
5-6	0.412 (0.692)	- -	- -

The expected hazard rate is obtained through Equation (15), which is defined using the exponential hazard function for the dataset mentioned above. The life expectancy of a rating, indicating the elapsed time in reaching the next rating is obtained using Equation (16). The effect of CMR on deterioration speed is analyzed for minimum and maximum levels of the explanatory variable. The expected deterioration path can be represented by a graph describing the average deterioration process during the life expectancy of the rating (from the time the rating is reached to the time the next rating is attained). The expected deterioration path of pavement for monsoon using EBK3D interpolation is illustrated in Figure 5.

The findings indicate that both traffic and environmental factors, i.e., CMR in this study, significantly contribute to pavement deterioration. The deterioration process is modeled using the positive values of the unknown parameter β for AADT and CMR. With EBK3D interpolation, the average pavement life expectancy is estimated at 4.22 years, incorporating AADT and CMR as explanatory variables. In Figure 5, the effect of monsoon indicates there is a significant reduction of 38.75% of the service life, which is acceptable and justifiable.
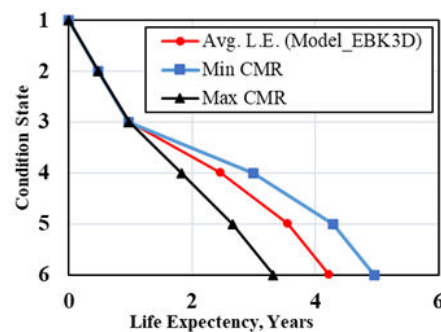
Figure 5. Expected deterioration path of pavement for monsoon using EBK3D.

6. Discussion

The results show the significant impact of traffic and environmental factors on road pavement deterioration. Referring to Table 4, the estimated value of β_{i1} for the traffic parameter shows the deterioration action on the pavement till the pavement is in a satisfactory condition. This deterioration process is relatable to real-world conditions. The negative values of β_{i1} for fair, poor, and bad conditions indicate that with an increase in traffic, the condition of the pavement will be improved, which is not acceptable, hence these values are excluded from the pavement deterioration model. Similarly, the estimated value of β_{i2} for the environmental parameter, i.e., CMR expressed in mm, indicates accelerated deterioration on the pavement in the satisfactory, fair, and poor condition states. This can be interpreted as when the pavement surface is in a good to satisfactory condition, the monsoon rain will safely drain off the pavement surface, which will not trigger the bituminous pavement failure mechanism. The average deterioration rates and the average life expectancies (in years) for different condition states are known. This information offers a practical time frame for planning efficient inspection intervals and maintenance strategies. From this study, the effect of monsoon is estimated in Figure 5 for different condition states, and the results show that the monsoon factor contributes to a significant 38.75% reduction of pavement service life.

In the context of DOR, periodic maintenance, along with combined maintenance activities, is carried out to keep the pavement in fair to good condition and prolong the life expectancy of the pavement. From the study, referring to Figure 5, the average life expectancy of bituminous pavement in Nepal is 4.22 years. If we assume that after periodic maintenance, the pavement will be reinstated to the best condition state, i.e., condition state 1, then, under the action of traffic and monsoon it will deteriorate and reach its absorbing state (J) in approximately 4 years. From this, it can be inferred that the current practice of periodic maintenance for resealing bituminous pavement at intervals of 5 to 8 years regardless of pavement deterioration rate, may be too long for roads exposed to high monsoon. As a result, the pavement may reach a condition state that cannot be restored to a good condition through periodic maintenance alone, ultimately requiring more costly maintenance solutions like rehabilitation or reconstruction [7].

Referring to Figure 5, the average pavement deterioration curves indicate that the pavement deterioration rate for Nepal is high considering the traffic and environmental factors. The current practice of reactive maintenance may not be sufficient for extending the service life of the pavement and reducing the life cycle cost in the long term. The introduction of a preventive maintenance strategy to supplement periodic maintenance could be an effective approach for bituminous pavement with higher CMR, where periodic maintenance alone may not restore the pavement to the expected good condition.

7. Conclusions

This research presents a comprehensive approach for integrating environmental data into pavement deterioration modeling using Markov deterioration hazard models. The key achievements of this study are as follows:

1. Integrating monsoon rainfall effects on pavement performance in Nepal: a Markov deterioration model is presented using SDI and incorporating monsoon rainfall as a key environmental factor.
2. Comparison of interpolation methods for rainfall estimation: by comparing the IDW and EBK3D interpolation techniques, we found that the EBK3D method provided a more accurate value for CMR, as supported by the lower MAE, RMSE, and MBE values.

3. Quantification of CMR on pavement deterioration: the study found that CMR accelerates pavement deterioration, reducing service life by approximately 38.75% in Nepal, and suggests better maintenance planning before and after the monsoon.

4. Practical Implications for road asset management: The findings demonstrate that geostatistical methods capable of accounting for spatial dependency, such as EBK3D, can enhance the accuracy of models that incorporate environmental factors like monsoon. These results suggest that road agencies like DOR should consider using more advanced interpolation methods like EBK3D when developing predictive models for pavement management, particularly in regions where environmental variables play a critical role in pavement performance.

While this study provides valuable insights into pavement deterioration modeling using a Markov hazard framework with environmental data, there are some limitations to consider. First, the accuracy of the model heavily relies on the quality of the input data. In this study, CMR data were the sum of daily monsoon values from June–September; however, the monsoon period may vary. Any inaccuracies due to early or delayed monsoon can give inaccurate values, which may affect the interpolation and model performance. Second, this study considered only cumulative monsoon rainfall as the environmental factor. Although rainfall is a critical factor, other environmental variables such as temperature fluctuations, freeze–thaw cycles, and soil type may also contribute significantly to pavement deterioration.

However, future studies can enhance the model by including other environmental and climatic factors such as temperature, freeze-thaw cycles, and humidity. This would provide a more comprehensive understanding of how different environmental conditions jointly affect pavement deterioration. Expanding the model to incorporate these variables could lead to improved predictions and more effective pavement management strategies.

The model can also be checked for different types of pavements (e.g., rigid, composite) and different regions of Nepal (e.g., plains, hills, and mountains) to evaluate its applicability and effectiveness in various contexts. Testing the model to varied topographies and pavement types will help in understanding how local conditions influence the deterioration process and will support the development of region-specific maintenance guidelines. These enhancements will contribute to more comprehensive pavement deterioration models, supporting infrastructure planning and resource allocation for effective road asset management.

Author Contributions: Conceptualization, M.M.S., K.S., F.O., A.A.A. and K.K.; methodology, M.M.S., K.S., F.O., A.A.A. and K.K.; software, M.M.S., K.S., F.O., A.A.A. and K.K.; formal analysis, M.M.S.; investigation, M.M.S.; resources, M.M.S.; data curation, M.M.S.; writing—original draft preparation, M.M.S.; writing—review and editing, M.M.S., K.S., F.O., A.A.A. and K.K.; supervision, K.K. All authors have read and agreed to the published version of the manuscript.

Data Availability Statement: The data used in this study are available from the corresponding author upon reasonable request.

Conflicts of Interest: The authors declare no conflicts of interest.

References

1. World Bank. Climate Change Knowledge Portal. 2023. Available online: https://climateknowledgeportal.worldbank.org/ (accessed on 6 October 2023).
2. Dahal, R.K. Rainfall-induced Landslides in Nepal. *Int. J. Jpn. Eros. Control Eng.* **2012**, *5*, 1–8. [CrossRef]
3. Nayava, J.L. Heavy Monsoon Rainfall in Nepal. *Weather* **1974**, *29*, 443–450. [CrossRef]
4. American Association of State Highway and Transportation Officials. *Pavement Management Guide*; American Association of State Highway and Transportation Officials: Washington, DC, USA, 2012.
5. Tsuda, Y.; Kaito, K.; Aoki, K.; Kobayashi, K. Estimating Markovian Transition Probabilities for Bridge Deterioration Forecasting. *JSCE* **2006**, *23*, 241–256. [CrossRef]
6. Department of Roads (DOR). DOR Website. 2022. Available online: https://www.dor.gov.np/home (accessed on 4 January 2023).
7. Department of Roads (DOR); Maintenance Branch. Standard Procedure for Periodic Maintenance Planning. 2005. Available online: https://www.dor.gov.np/home/publications (accessed on 20 February 2025).
8. Hossain, A.R.M.A.; Islam, A.; Khan, M.U. Strategic Direction ST4: Asset Management—Technical Inputs to Decision Making. In Proceedings of the 23rd World Road Congress, Paris, France, 17–22 September 2007; Available online: https://proceedings-paris2 007.piarc.org/ressources/files/5/RN-bd4-E.pdf (accessed on 20 February 2025).
9. Jain, S.S.; Aggarwal, S.; Parida, M. HDM-4 Pavement Deterioration Models for Indian National Highway Network. *J. Transp. Eng.* **2005**, *131*, 623–631. [CrossRef]
10. Thube, D.T. Highway Development and Management Model (HDM-4): Calibration and adoption for low-volume roads in local conditions. *Int. J. Pavement Eng.* **2013**, *14*, 50–59. [CrossRef]
11. Han, D.; Kaito, K.; Kobayashi, K. Application of Bayesian Estimation Method with Markov Hazard Model to Improve Deterioration Forecasts for Infrastructure Asset Management. *KSCE J. Civ. Eng.* **2014**, *18*, 2107–2119. [CrossRef]
12. Kobayashi, K.; Kaito, K.; Lethanh, N. A Bayesian Estimation Method to Improve Deterioration Prediction for Infrastructure System with Markov Chain Model. *Int. J. Archit. Eng. Constr.* **2012**, *1*, 1–13. [CrossRef]
13. Wang, W.; Wang, L.; Miao, Y.; Cheng, C.; Chen, S. A survey on the influence of intense rainfall induced by climate warming on operation safety and service life of urban asphalt pavement. *J. Infrastruct. Preserv. Resil.* **2020**, *1*, 4. [CrossRef]
14. Talchabhadel, R.; Aryal, A.; Kawaike, K.; Yamanoi, K.; Nakagawa, H. A comprehensive analysis of projected changes of extreme precipitation indices in West Rapti River basin, Nepal under changing climate. *Int. J. Climatol.* **2021**, *41* (Suppl. 1), E2581–E2599. [CrossRef]
15. World Bank. *Road Deterioration in Developing Countries, Causes and Remedies*; World Bank: Washington, DC, USA, 1988; Available online: https://documents.worldbank.org/en/publication/documents-reports/documentdetail/722851468162562433/Road-deterioration-in-developing-countries-causes-and-remedies (accessed on 26 February 2025).
16. Kodippily, S.; Yeaman, J.; Henning, T.; Tighe, S. Effects of extreme climatic conditions on pavement response. *Road Mater. Pavement Des.* **2020**, *21*, 1413–1425. [CrossRef]
17. Alnaqbi, A.; Zeiada, W.; Al-Khateeb, G.G. Machine learning modeling of pavement performance and IRI prediction in flexible pavement. *Innov. Infrastruct. Solut.* **2024**, *9*, 385. [CrossRef]
18. DHM (Department of Hydrology and Meteorology). 2024. Available online: https://www.dhm.gov.np/ (accessed on 5 November 2024).
19. Chen, F.W.; Liu, C.W. Estimation of the spatial rainfall distribution using inverse distance weighting (IDW) in the middle of Taiwan. *Paddy Water Environ.* **2012**, *10*, 209–222. [CrossRef]
20. Krivoruchko, K. Empirical Bayesian Kriging Implemented in ArcGIS Geostatistical Analyst. 2012. Available online: https://www.researchgate.net/publication/286305814_Empirical_bayesian_kriging_implemented_in_ArcGIS_geostatistical_analyst (accessed on 20 February 2025).
21. Esri. ArcGIS Documentation. Empirical Bayesian Kriging 3D (Geostatistical Analyst)—ArcGIS Pro. Available online: https://pro.arcgis.com/en/pro-app/latest/tool-reference/geostatistical-analyst/empirical-bayesian-kriging-3d.htm (accessed on 20 October 2024).
22. ESRI. ArcGIS® 9 Using ArcGIS® Geostatistical Analyst. Esri: Redlands, CA, USA, 2001; Available online: https://downloads2 .esri.com/support/documentation/ao_/Using_ArcGIS_Geostatistical_Analyst.pdf (accessed on 20 February 2025).
23. Esri. ArcGIS Documentation. Kriging (Geostatistical Analyst)—ArcGIS Pro. Available online: https://pro.arcgis.com/en/pro-app/latest/tool-reference/3d-analyst/how-kriging-works.htm (accessed on 1 November 2024).
24. Swara, H.R.; Nur, I.; Ilyas, A.; Widodo, S. Analysis of Empirical Bayesian Kriging Methods for Optimization of Measured Resources Estimation of Laterite Nickel. *IOP Conf. Ser. Earth Environ. Sci.* **2023**, *1134*, 012037. Available online: https://iopscience.iop.org/article/10.1088/1755-1315/1134/1/012037 (accessed on 26 February 2025). [CrossRef]
25. Department of Roads (DOR); MRCU. Road Pavement Management Discussion Paper. 1995. Available online: https://dor.gov.np/home/publication/general-documents (accessed on 10 November 2022).
26. Department of Hydrology and Meteorology. Meteorological Observations. 2023. Available online: https://www.dhm.gov.np/hydrology/rainfall-watch-map (accessed on 29 June 2023).

27. Willmott, C.J.; Matsuura, K. Advantages of the mean absolute error (MAE) over the root mean square error (RMSE) in assessing average model performance. *Clim. Res.* **2005**, *30*, 79–82. Available online: https://www.int-res.com/abstracts/cr/v30/n1/p79-82 (accessed on 26 February 2025). [CrossRef]

28. Lancaster, T. *The Econometric Analysis of Transition Data*; Cambridge University Press: Cambridge, UK, 1990.

29. Department of Roads. Road Register 2023. 2023. Available online: https://armp.dor.gov.np/ (accessed on 23 June 2023).

30. DOR; MOPIT. Nepal's National Experience on Developing Sustainable and Resilient Road Infrastructure Network. 2023. Available online: https://www.unescap.org/sites/default/d8files/event-documents/Policy%20Segment,%20Session%202_02%20Nepal.pdf (accessed on 26 February 2025).

31. Smith, H.R.; Rolt, J.; Ford, W.G. *Overseas Road Note 3 (2nd Edition) A Guide to Surface Dressing in Tropical and Sub-Tropical Countries ORN 3*, 2nd ed.; TRL Ltd.: Crowthorne, UK, 2021.